An integral activity-based protein profiling (IABPP) method for higher throughput determination of protein target sensitivity to small molecules

Chathuri J. Kombala[1],[†] Agne Sveistyte[1],[†] Tong Zhang[1], Leo J. Gorham[1], Gerard X. Lomas[1], John T. Melchior[1], Priscila M. Lalli[1], Vanessa L. Paurus[1], Stephen J. Callister[1], Aaron T. Wright[2,3],[*] Vivian S. Lin[1*]

[†]Equal contribution

[1] Biological Sciences Division, Pacific Northwest National Laboratory, Richland, Washington, 99354, United States

[2] Department of Biology, Baylor University, Waco, Texas, 76798 USA

[3] Department of Chemistry and Biochemistry, Baylor University, Waco, Texas, 76798 USA

Corresponding Author

*a_wright@baylor.edu, *vivian.lin@pnnl.gov

Abstract

Activity-based protein profiling (ABPP) is a chemoproteomic technique that uses chemical probes to label active enzymes selectively and covalently in complex proteomes. Competitive ABPP, which involves treatment of the active proteome with an analyte of interest, is especially powerful for profiling how small molecules impact specific protein activities. Advances in higher throughput workflows have made it possible to generate extensive competitive ABPP data across various biological systems and treatments, making this approach highly appealing for characterizing shared and unique proteins affected by perturbations such as drug or chemical exposures. To use the competitive ABPP approach effectively to understand potential adverse effects of chemicals of concern, a wide range of concentrations may be needed, particularly for

chemicals that may lack toxicity data. In this work, we present an integral competitive ABPP method that enables target sensitivity differentiation across a wide range of concentrations for the model organophosphate (OP), paraoxon. Using previously developed OP-ABPs, we optimized conditions for tandem mass tag (TMT) multiplexing of ABPP samples and compared conventional competitive ABPP involving discrete samples at various paraoxon concentrations with pooling of samples across that same concentration range. The results show that small vs. large differences in integral intensities for the competitive sample can be used to distinguish low vs. high sensitivity proteins, respectively, without increasing the overall number of samples. We envision the integral ABPP method will provides a means to screen diverse chemicals more rapidly to identify both highly sensitive and less sensitive protein targets.

Introduction

Activity-based protein profiling (ABPP) is a powerful chemoproteomic technique that enables specific identification of functionally active proteins in mixed proteomes. ABPP uses small molecule tools called activity-based probes (ABPs) that covalently react with target enzymes in a mechanism-specific manner. While ABPs must be individually synthesized for different enzyme classes, competitive ABPP, in which a sample is pretreated with a chemical of interest to identify changes in activity (**Figure 1A**), enables assessment of the functional impact of chemicals in diverse biological samples. Competitive ABPP has been used widely to evaluate the interaction of protein targets with chemicals ranging from drugs,[1-3] pesticides,[4-6] pollutants, and more.[7, 8] However, the selection of competitor concentrations remains a critical consideration for determining the practical significance of proteins identified using this method, bringing to mind the toxicology adage *Sola dosis facit venenum* ("the dose makes the poison").[9] Unrealistically high concentrations of chemicals may not reflect biologically relevant scenarios, while both high and low doses may represent important but different types of exposures that may affect distinct cellular pathways. Metabolism in the body also complicates our ability to perform these *in vitro* ABPP studies for chemicals of interest in a manner that can be readily translated to understanding the *in vivo* molecular level effects. Thus, competitive ABPP to inform our pharmacological or toxicological understanding of protein sensitivities toward a chemical ideally would be performed over a wide, biologically relevant concentration range.

The ongoing emergence of thousands of chemicals of concern has created a great need for target identification to understand potential mechanisms of toxicity, but limitations with sample preparation and analysis throughput make investigation of many concentrations for multiple chemicals a practical challenge in terms of cost and time for competitive ABPP. For a new chemical of concern, the relevant concentration range for toxicity may be unknown, and individual proteins may display widely disparate sensitivities. Recent advancements in streamlining and automation of chemoproteomic sample preparation workflows have now made it possible to generate samples in a higher throughput manner compared to traditional manual methods.[10-12] Despite these significant improvements in sample preparation, chemoproteomic sample analysis by liquid chromatography tandem mass spectrometry (LC-MS/MS) remains a significant bottleneck. The availability of isobaric labeling using tandem mass tag (TMT) reagents to multiplex LC-MS/MS samples up to 18-fold[13] has provided avenues to increasing throughput of ABPP data generation. TMT labeling has been demonstrated in combination with various chemoproteomic tools, including cysteine- and other reactive probes for nucleophilic residues,[14, 15] metabolic labeling probes,[16] and ABPs[17, 18] However, requirements for TMT plex design impose practical limitations on how many samples can be multiplexed at a time (**Figure 1B**). Performing competitive ABPP for multiple competitor concentrations across multiple chemicals of concern therefore remains costly in terms of instrument run times and resources required to process each individual sample.

To increase analytical throughput without compromising on the number of concentrations that can be profiled, we explored an integral competitive ABPP method (**Figure 1C**), inspired by the proteome integral solubility assay (PISA) approach developed for thermal proteome profiling of protein structure.[19] The integral approach enables profiling of a broad competitor concentration range, where pooling samples collapses the competitor samples into a single protein sample for enrichment. After optimizing a TMT labeling protocol for OP-ABPs in mammalian tissue lysates, we demonstrate integral competitive ABPP using the fluorophosphonate ABP FP2 to evaluate the impact of the OP pesticide paraoxon on serine hydrolase functions in rodent tissue homogenates.[20] This approach dramatically decreases the number of samples that must be enriched and TMT labeled, yielding significant savings in terms of sample preparation time and reagent costs. We envision that this approach will allow for higher throughput screening of chemicals of interest while also providing quantitative data that can distinguish highly sensitive protein targets from

less sensitive proteins. We anticipate that the increased depth of data that can be achieved using this method will deliver important new insights into the biological impact of specific proteins in diverse systems, from pharmaceutical research to toxicology.

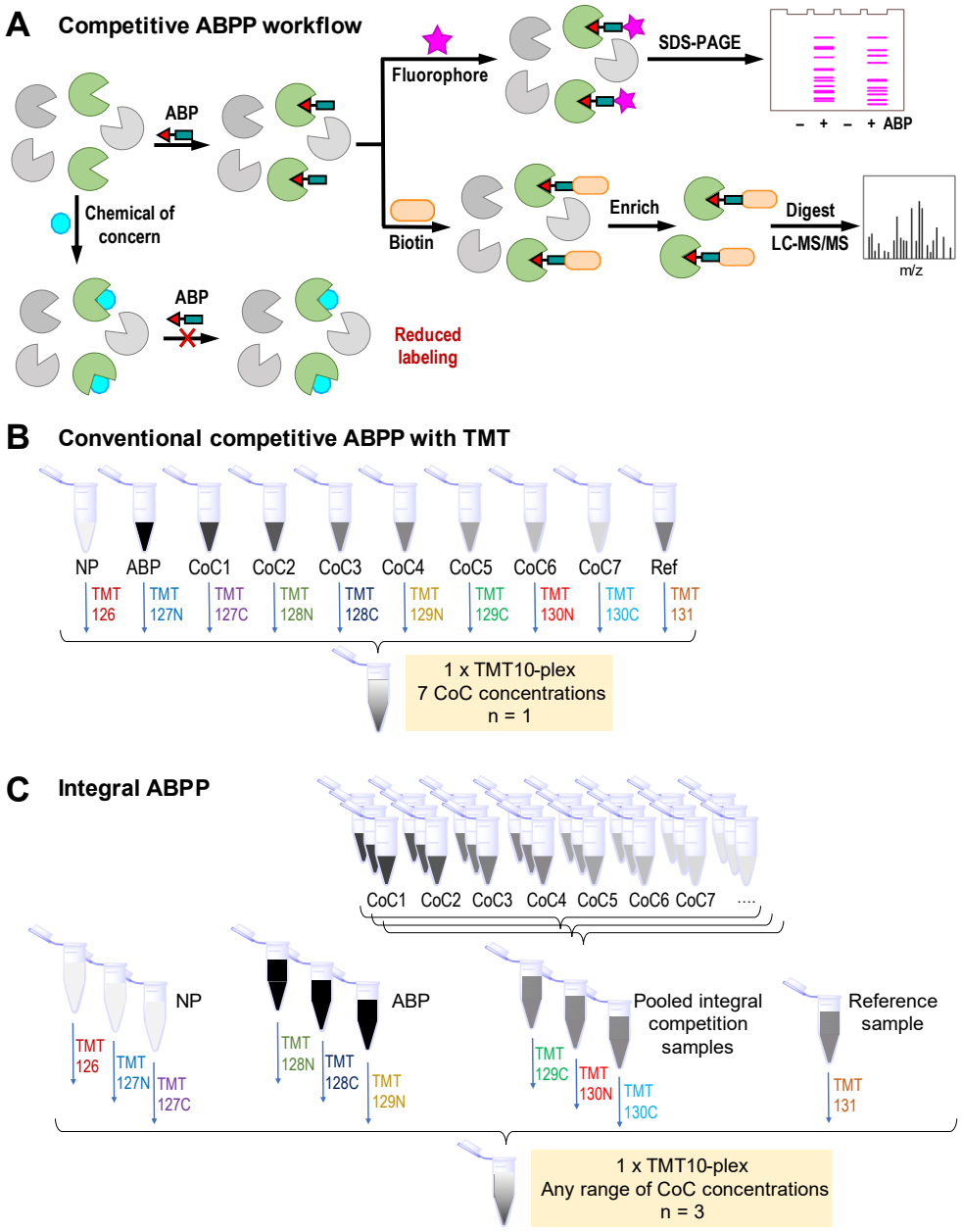

Figure 1. **(A)** Competitive activity-based protein profiling (ABPP) workflow for identifying proteins in a complex proteome that are functionally impacted by a chemical of concern (CoC). Treatment of active proteins with the chemical of concern blocks binding of the activity-based

probe (ABP), reducing detection of probe-labeled protein targets. Conventional (**B**) and integral competitive ABPP (**C**) workflows, which include ABP only and "no probe" (NP) positive and negative controls, respectively. Tandem mass tag (TMT) labeling enables sampling multiplexing for both approaches, while pooling competition samples across a range of concentrations increases throughput for the integral ABPP.

Methods

Materials

FP2 probe was synthesized according to Wiedner et al.[20] Probe was prepared in dry DMSO and stored at -80 °C as single-use 50 mM aliquots to minimize freeze-thaw cycles. Chemicals and reagents were purchased from ThermoFisher, VWR, and Vector Labs, and used without further purification.

Conventional competitive ABPP

Mouse lung lysate (800 µL, 2 mg/mL total protein concentration) was added to deep well plates (1 mL) and treated with ethanol (vehicle) or different concentrations of paraoxon in ethanol (0.01, 0.05, 0.1, 0.2, 0.5, 1, 5, 10 µM) separately at 37 °C for 30 min. FP2 probe (10 µM) was added to each well and incubated at 37 °C for 1 h on a thermoshaker. No probe (NP) control (DMSO; 2% v/v) and probe only control reactions were also prepared. All samples were prepared in triplicate.

Integral competitive ABPP

Mouse lung lysate (100 µL, 2 mg/mL total protein concentration) was added to deep well plates (1 mL) and treated with eight different concentrations of paraoxon in ethanol (0.01, 0.05, 0.1, 0.2, 0.5, 1, 5, 10 µM) separately at 37 °C for 30 min. FP2 probe (10 µM) was added to the treated lysates and incubated at 37 °C for 1 h on a plate thermoshaker. Each of the eight different paraoxon concentrations treated lysate reactions (100 µL) were pooled to have integral competitive proteome (total volume 800 µL). No probe control (DMSO) and probe only control reactions also

carried out in 8 x 100 µL fractions and pooled. All integral competitive ABPP samples were prepared as technical replicates of four. No probe and probe only reactions were prepared in triplicate.

Proteomics sample preparation

Click chemistry. After probe incubations were complete, all probe-labeled protein lysates were subjected to copper-catalyzed click chemistry by adding biotin azide (30 µM), followed by sodium ascorbate (5 mM), THPTA (2.8 mM), and copper sulfate (4 mM). The reactions were incubated in the dark for 1 h at 37 °C on a thermal shaker. Following the incubation, excess rhodamine was removed by precipitating the protein using cold methanol (1:4 v/v, sample:methanol). Methanol added samples were placed in the -80 °C freezer for overnight followed by centrifugation at 10,500 × g at 4 °C for 10 min, and the supernatant was discarded. The samples were allowed to air dry with caps open for about 15 min. Proteins were resolubilized by adding SDS in 1x PBS (1.2%, 520 µL), heated at 95 °C for 2 min, and sonicated 12 sec, 1 sec on/off, with 60% amplitude. The samples were centrifuged at 10,500 × g at 4 °C for 5 min to remove insoluble material. Supernatant was carefully transferred to new centrifuge tubes leaving any pellet behind. The solubilized protein concentration was determined by BCA assay and concentration was normalized using 1.2% SDS in PBS. Samples were normalized to 1200 µg of total protein in 650 µL volume.

Samples were enriched on streptavidin-agarose resin, reduced and alkylated, and trypsin digested. Detailed methods for these steps are provided in the Supporting Information.

Tandem mass tag (TMT) labeling. Experiments testing TMT labeling conditions for optimization of methods is described in the Supporting Information. Peptides were removed from the -80 °C freezer and allowed to warm to room temperature. Then, the samples were reconstituted in 20 µL of 50% acetonitrile in HPLC grade water. For TMT 10-plex, the isobaric label reagents (Fisher PI90406) were reconstituted in anhydrous acetonitrile to a 17 µg/µL concentration solution per tag, and 3 µL was added to the corresponding sample. For TMT 18-plex, the isobaric label reagents (Fisher A52047) were reconstituted in anhydrous acetonitrile to 20 µg/µL per tag, and 2.5 µL was added to the corresponding sample. The samples were then vortexed, briefly centrifuged, and then incubated at 25 °C for 1 hour at 400 rpm. The reactions were then quenched by adding 2

μL of 5% hydroxylamine and incubated for 15 minutes at 25 °C and 400 rpm. After quenching, equal volumes from each sample in the TMT10-plex were combined. The combined samples were completely dried in a SpeedVac concentrator. After the samples were dry, they were reconstituted in 100 μL of 8% formic acid/5% acetonitrile in HPLC grade water.

LC-MS/MS

ABPP samples were analyzed using a Waters nanoAcquity ultra performance liquid chromatography (UPLC) system connected to a Q Exactive Plus Orbitrap mass spectrometer (Thermo Scientific, San Jose, CA). Samples were loaded into a precolumn (150 μm i.d., 4 cm length, packed in-lab with Jupiter C18 packing material, 300 Å pore size, 5 μm particle size; Phenomenex, Torrance, CA, USA) using mobile phase A (0.1% formic acid in water). The separation was carried out in a LC column (packed in-lab into an empty self pack NanoLC column (CoAnn Technologies, Richland, WA) 75 μm i.d., 30-cm column with Waters BEH C18 packing material, 130-Å pore size, 1.7 μm particle size (Waters Corporation, USA)) at a flow rate of 200 nL/min using a 60 min gradient of 1-75% mobile phase B (acetonitrile + 0.1% formic acid) for mouse lung tissue IABPP samples. To prevent carryover, the column was washed with 95-50% mobile phase B for 20 min and equilibrated with 1% mobile phase B for 30 min before the next sample injection. The mass spectrometer source was set at 2.2 kV, and the ion transfer capillary was heated to 300 °C. The data-dependent acquisition mode was employed to automatically trigger the precursor scan and the MS/MS scans. The MS1 spectra were collected at a scan range of 300-1800 m/z, a resolution of 70,000, an automatic gain control (AGC) target of 3×10^6, and a maximum injection ion injection time of 20 ms. For MS2, top 12 most intense precursors were isolated with a window of 1.5 m/z and fragmented by higher-energy collisional dissociation (HCD) with a normalized collision energy at 30%. The Orbitrap was used to collect MS/MS spectra at a resolution of 17,500, a maximum AGC target of 1×10^5, and maximum ion injection time of 50 ms. Each parent ion was fragmented once before being dynamically excluded for 30 s.

Data analysis

The three TMT10 datasets for conventional ABPP were searched using MSGF+[24] against the mouse protein database (UniProt for *Mus musculus*, downloaded on 03-01-2024) with the following parameters: parent ion tolerance of 20 ppm; methionine oxidation (+15.9949 Da) as a dynamic modification; cysteine alkylation (+57.0215 Da) and TMT-labeling of lysine and N-terminal peptides (+229.1629 Da) as static modifications. The same searching parameters were used for the TMT18 dataset for the IABPP experiment except the TMT mass was set to +304.207146. The MSGF+ search results were linked to the MS/MS Automated Selected Ion Chromatogram generator (MASIC)[25] reporter ion quantification and aggregated to protein level using PlexedPiper (https://github.com/vladpetyuk/PlexedPiper). To identify target proteins in the conventional competitive ABPP datasets, the following criteria were used: 1) quantified in all three TMT sets; 2) the signal to noise (S/N), defined as the TMT intensity ratio between the FP2 ABP channel and the "no probe" control, was > 2 in at least one of the three replicates; and 3) the competition ratio (CR), defined as the TMT intensity ratio between the paraoxon-treated samples and the ABP channel, was < 0.8. Since paraoxon of eight concentrations were included in each TMT set, CR was determined by calculating the area under the curve (AUC) of the plot between competitor concentrations (x axis) and relative protein abundance (y axis, Figure 3). Relative protein abundance was obtained by scaling the TMT intensity of competitor channels to that of the ABP channel. For each protein, a response curve was constructed by connecting the relative abundance across nine experimental conditions (ABP and competitor concentrations 1-8). No curve fitting was performed. The response curve was then enclosed by two vertical lines (one intersecting the ABP and the other at the highest concentration) and a horizontal line at y= 0, forming a polygon (light blue shade in Figure 3). The area of this polygon was subsequently calculated using Gauss's area formula in R. For the IABPP datasets, S/N and CR were calculated using the mean of replicates within the same TMT set, and the same cutoffs were used to identity target proteins.

Results

To enable higher throughput analyses of ABPP samples, we optimized TMT labeling conditions for OP-ABPs using different TMT tag to peptide ratios (see Supporting Information). From the three TMT conditions tested, TMT 50:1, in which TMT tag to peptide ratio was 50:1

(w/w), produced the best results overall. While TMT 10:1 resulted in the highest number of scans searched, it was outperformed by TMT 50:1 in the number of peptide-to-spectrum matches (PSMs), as well as unique peptide and protein identifications (**Figure 2A**); TMT50 conditions resulted in 95% labeling efficiency (**Figure 2B**). Even though TMT 100:1 resulted in a modestly higher labeling efficiency than TMT 50:1, it led to inferior number of scans and PSMs, as well as fewer unique peptide and protein identifications. Overall, fewer unique peptides and proteins were identified by ABPP-TMT compared to the label-free ABPP approach, although many of the shared protein targets identified by both methods represented the "strongest" targets, i.e. those with the highest fold changes for competitive ABPP (**Figure 2C-D**).

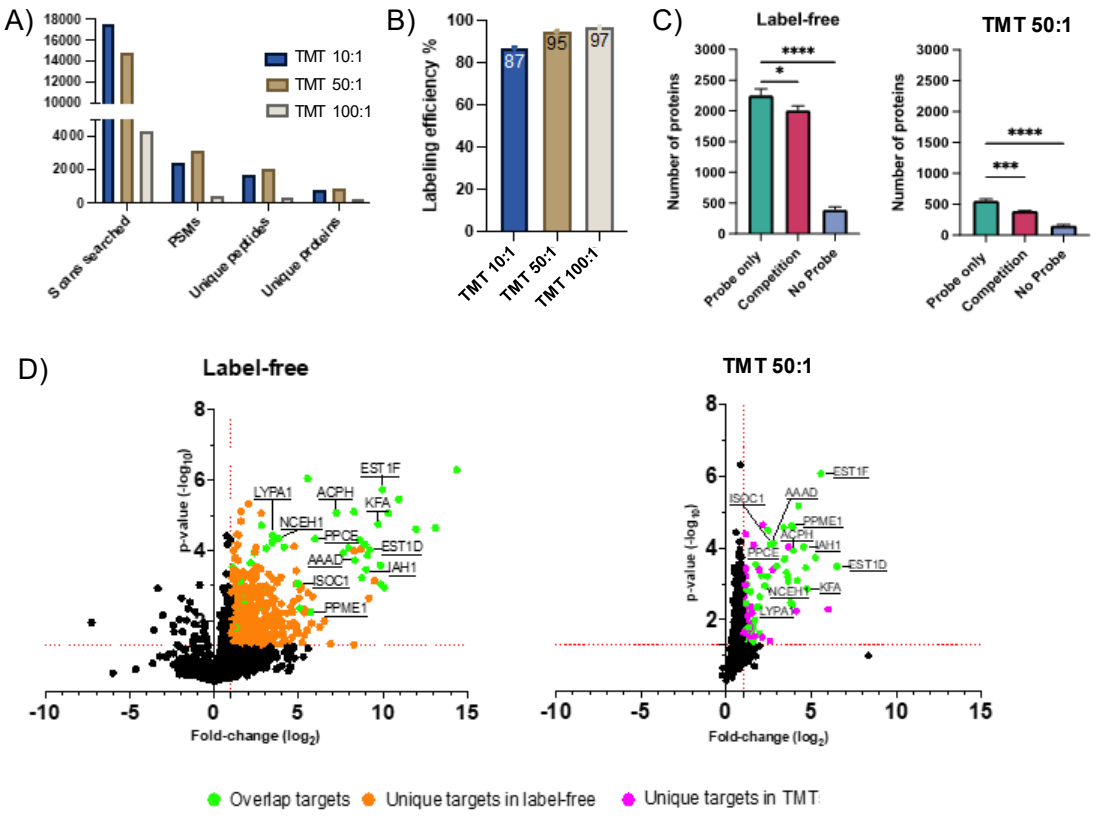

Figure 2. Comparison of competitive ABPP for paraoxon targets in rat liver homogenates using a label-free approach or TMT labeling. A) MS-GF+ outputs for TMT tag to peptide w/w ratios of 10:1 (TMT 10:1), 50:1 (TMT 50:1), and 100:1 (TMT 100:1). Peptide to spectrum matches (PSMs), unique peptides, and unique proteins were filtered at MS-GF+ < $1x10^{-10}$. Bars each represent calculated values for one TMT 10plex containing one pooled reference sample and three

replicates from the three ABPP groups ("Probe," "Competition," and "No Probe") prior to de-multiplexing. B) Calculated TMT labeling efficiency for each tested ABPP-TMT condition. C) Numbers of proteins identified in each of the three ABPP groups for label-free and TMT 50:1 methods. Adjusted P values for *, ***, and **** were < 0.05, < 0.001, and < 0.0001, respectively. D) Volcano plots of proteins identified for the label-free and TMT 50:1 methods in paraoxon competition ABPP labeling of rat liver homogenates. Only proteins for which a Welch's t-test could be performed are shown; presence/absence data are presented in Figure S4. Points above horizontal and to the right of vertical red lines represent statistically significant protein targets (horizontal line adjusted *p* value = 0.05; vertical line fold-change = 2). Selected known protein targets of paraoxon are labeled.

Conventional competitive ABPP was performed using the optimized TMT 50:1 labeling conditions in mouse lung tissue homogenate across a nanomolar to micromolar range of paraoxon followed by labeling with FP2. Paraoxon concentrations were selected based on fluorescent gel analysis of FP2 labeling in mouse lung, which showed various protein bands that decreased in intensity over this concentration range (**Figure 3B**). Conventional competitive ABPP performed at these discrete paraoxon concentrations yielded individual data points that clearly showed protein sensitivity differences at higher or lower concentrations of paraoxon. To compare conventional ABPP to integral ABPP, we calculated the area under the curve (AUC) for the conventional ABPP plots (**Figure 3D**). We used an AUC cutoff of 0.8 to identify proteins that were competed by paraoxon at the tested concentration range. More sensitive protein targets such as butyrylcholinesterase (CHLE) had smaller AUC values, and less sensitive protein targets such as monoacylglycerol lipase (MGLL) had larger AUC. Acyl-CoA thioesterase 1 (ACOT1), which is a serine hydrolase and has been previously identified using other fluorophosphonate ABPs,[26, 27] had a calculated AUC of 0.89 and was therefore not identified as a significant paraoxon protein target in these experiments.

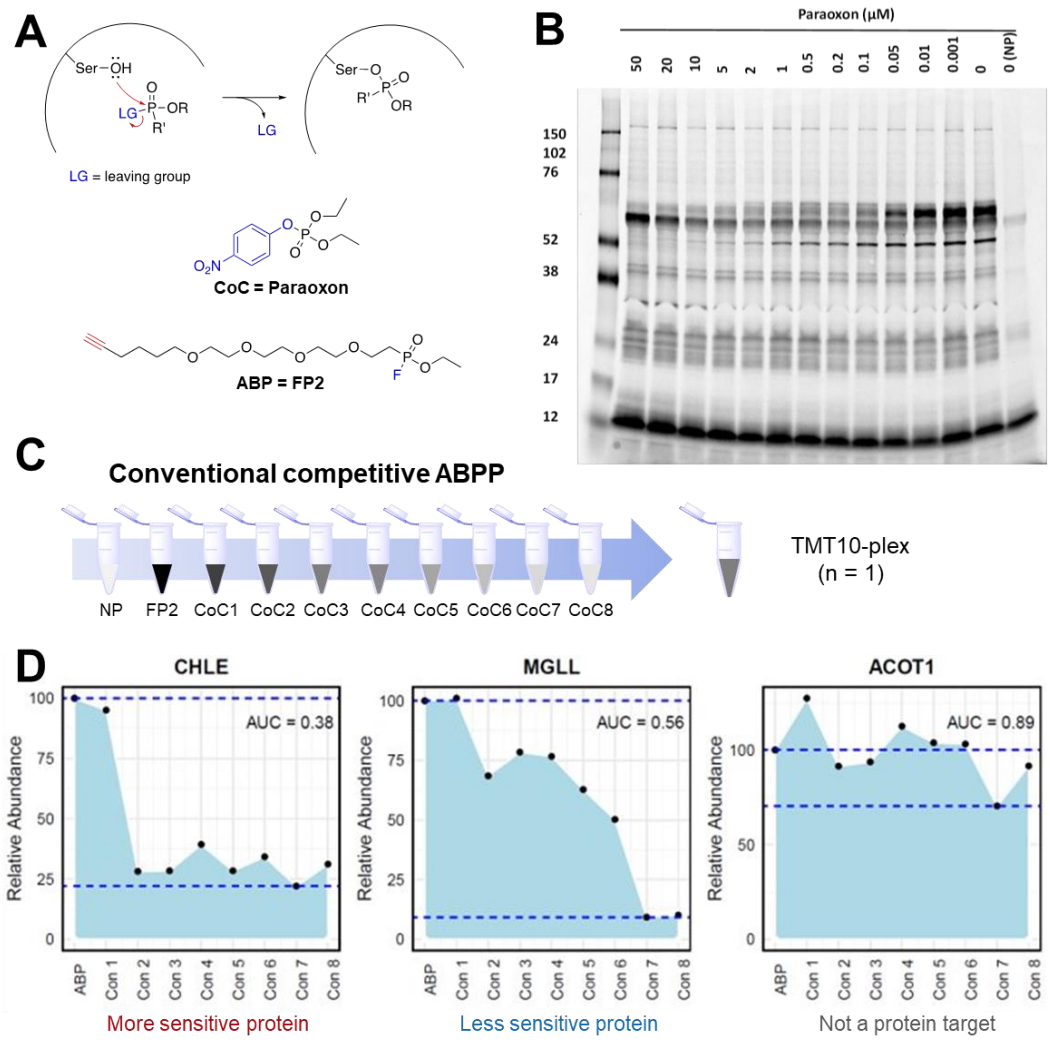

Figure 3. Conventional competitive ABPP. (A) Mechanism of enzyme inhibition by OP toxicants and structures of chemical of concern (CoC) and activity-based probe (ABP) used for comparison of competitive ABPP methods. (B) Fluorescence gel image for FP2 (10 μM) labeling of mouse lung tissue lysate treated over a nanomolar to micromolar concentration range of paraoxon. Probe only (0 μM paraoxon) positive control and no probe (NP) negative control lanes represent highest and lowest fluorescence from FP2 labeling, respectively. (C) Conventional competitive ABPP study design, where each sample is a separate channel in a TMT plex. (D) Example conventional competitive ABPP results for selected protein targets displaying differential sensitivities toward paraoxon. Plots of relative abundance for probe only (ABP, with ethanol vehicle control), and paraoxon competitor at 8 different paraoxon concentrations in ascending order (0.01, 0.05, 0.1, 0.2, 0.5, 1, 5, 10 μM). Area under the curve (AUC) is quantified for each protein.

A comparison of the top protein targets from the conventional and the integral competitive ABPP approach showed overlap of 11 proteins known to be targets of organophosphates such as paraoxon (**Figure 4B**). In mouse lung tissue, we identified butyrylcholinesterase (CHLE) as a more sensitive protein target, along with several carboxylesterases (CES2G, EST1, EST1C, EST1D, EST1E, EST1F). Another well-known protein target of paraoxon, monoacylglycerol lipase (MGLL), was identified as a moderately sensitive protein target, while hormone-sensitive lipase (LIPS) was the weakest target identified in both ABPP methods. A comparison of conventional ABPP calculated AUC values with integral ABPP intensity differences showed good correlation (r = 0.89) between the shared 11 protein targets.

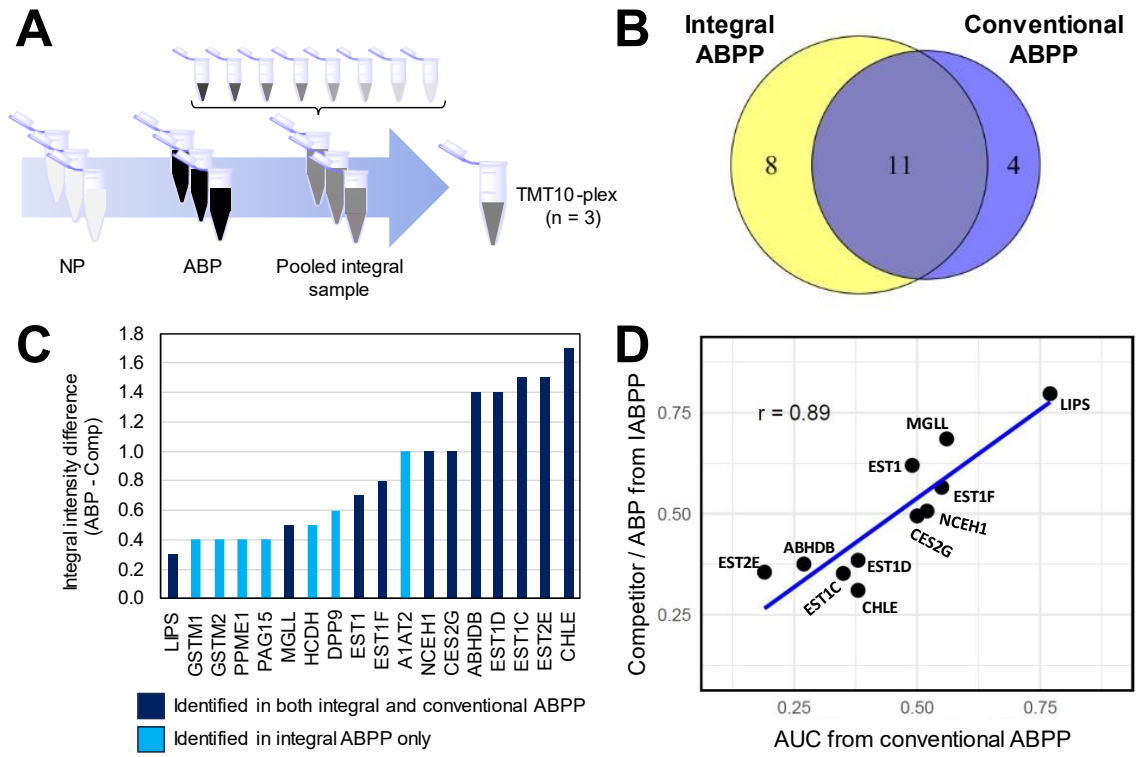

Figure 4. Integral ABPP (IABPP) results in mouse lung tissue homogenate for paraoxon. (A) IABPP allows for multiplexing of multiple replicates for pooled competition samples with no probe (NP) negative control and ABP positive control samples into a single sample. (B) Venn diagram of proteins significantly competed by paraoxon treatment (0.01, 0.05, 0.1, 0.2, 0.5, 1, 5,

10 µM) for IABPP and conventional ABPP methods (C) Selected proteins identified by the IABPP approach and their integral intensity differences between ABP and pooled competition samples across paraoxon treatment. (D) Correlation plot of integral intensity differences for IABPP and area under the curve (AUC) for conventional ABPP.

Of the eight proteins identified by integral ABPP but not conventional ABPP as statistically significant protein targets of paraoxon (**Figure 4B-C**), we found that 6 of these proteins were also observed in the conventional ABPP dataset but did not pass the criteria for paraoxon competition (AUC > 0.8) (**Figure S2**). Some of these proteins, such as protein phosphatase methylesterase 1 (PPME1), dipeptidyl peptidase 9 (DPP9), and lysosomal phospholipase A and acyltransferase (PAG15), are members of the alpha/beta hydrolase superfamily and contain catalytic serines.[27] These proteins were among those identified in our previous study using OP-ABPs with higher concentrations of paraoxon (50 µM) in rat brain and liver tissues.[5] Glutathione S-transferase mu 1 (GSTM1) and mu 2 (GSTM2), which were also identified by IABPP but not determined to be significant targets by conventional ABPP, were previously identified using OP-ABPs.[28]

Discussion

Chemoproteomic sample throughput has greatly benefitted from recent advancements in sample preparation workflow automation and isobaric tagging that places a specific "barcode" on peptides from a single sample, enabling multiplexing of multiple samples into a single LC-MS/MS run. Optimizing TMT labeling for our traditional ABPP workflow allows us to compare three technical replicates treated at eight concentrations of paraoxon with corresponding controls in just three total LC-MS/MS samples using a TMT 10plex. Our optimization of TMT labeling conditions for post-enriched ABPP samples indicated that a relatively higher ratio of TMT reagent to peptide was required for high TMT labeling efficiency, as recommended by Zecha et al. for peptide quantities below 10 micrograms.[13] Unlike global proteomics samples, post-enrichment ABPP samples are highly reduced in complexity and contain much lower quantities of peptide, making these samples more comparable to single cell or other limited protein samples than bulk global proteomics.[29] In our research, peptide quantitation of ABPP samples has typically yielded low

micrograms to hundreds of nanograms of peptide, depending upon the probe and biological system. TMT kit manufacturer's protocols describe labeling conditions for 10-25 micrograms of peptides and do not recommend using this assay for peptide mixtures that are less than 1 microgram, suggesting thorough optimization of TMT labeling for low peptide ABPP samples may still be a work in progress.

We performed a comprehensive evaluation of TMT labeling conditions for OP-ABPs in two types of rat tissues to ensure we could achieve high labeling efficiency and good proteome coverage while minimizing usage of these expensive reagents. Even though others have reported optimized methods for global proteomics that enable reduction of the TMT tag:peptide ratio to as low as 1:1 w/w,[13] we found that 50:1 yielded the best results for enriched OP-ABP samples containing low microgram quantities of protein. In 2022, Guo et al. published a protocol for TMT labeling of top-down proteomics samples that recommended a double labeling strategy using 4:1 TMT tag:peptide for limited samples[30] which may provide a means to reduce TMT reagent usage in future OP-ABPP studies. Overall, using a TMT10-plex enabled a 9-fold reduction in LC-MS samples, a critical improvement in terms of savings and instrument resources. Unsurprisingly, the label-free approach produced higher protein target identifications than TMT, as has been previously reported by systematic studies comparing these methods.[31] Nonetheless, the increased throughput of TMT labeling for ABPP, particularly for large numbers of samples, makes the ABPP TMT approach advantageous despite potential drawbacks with coverage and missingness.

In our previous work with OP-ABPs, label free competitive ABPP frequently yielded proteins which were completely competed by OP treatment at a single, high dose concentration.[5] Missing values in proteomics data are common and present a challenge for quantitative comparison across proteins, since a fold change value based on intensities cannot be calculated. While various data imputation methods have been explored for missing values in proteomics data, we still lack appropriate methods that can account for variance in peptide quantifications.[32] ABPP TMT yielded few proteins that were not observed in the competitor sample, i.e. fewer missing values, which has been previously noted for TMT labeling compared to label-free approaches.[33] Since the integral approach includes very low concentrations of competitor, we also anticipate that the pooled competitor sample is less likely than a single, high dose competitor sample to yield missing values for most proteins, unless the protein target is especially sensitive. In this study, no proteins had

missing values for the pooled competitor sample, and we were therefore able to calculate fold changes for all statistically significant protein targets. Thus, the integral approach is more robust than single, high dose competitor treatment for quantitative comparison of protein target sensitivity in these complex samples.

Proteins that were determined to be sensitive targets of paraoxon in mouse lung based on the integral ABPP method included many proteins known to be inhibited by paraoxon and other OPs. The reported IC_{50} value of paraoxon for mouse CHLE is 24 ± 2.8 nM,[34] while the paraoxon IC_{50} of mouse MGLL is about 100-fold higher, at 2 ± 1.1 μM.[35] Rodent carboxylesterases, which are known to be inhibited by various OPs,[36] may have a protective effect under certain exposure scenarios due to differences in reactivity between carboxylesterases and the primary target affecting OP toxicity, acetylcholinesterase.[37] Rodents also possess twenty carboxylesterases, due to tandem gene duplication, compared to the six human carboxylesterase genes.[38] Rodents can survive much higher OP doses compared to humans, and efforts to engineer carboxylesterase knockout mouse models have therefore been pursued for better animal to human translation.[38] Our integral ABPP work is consistent with these observations that carboxylesterases are both abundant and sensitive toward OPs in rodent tissues and highlights the potential utility of integral ABPP for characterizing protein target sensitivities across different protein targets, animal models, and chemicals of concern to assess mechanisms of toxicity in greater detail than previous possible.

There were several proteins known to have serine hydrolase functions that were labeled by the FP2 ABP but were not determined to be statistically significant protein targets of paraoxon at the concentration range tested through either integral or conventional competitive ABPP. We did not investigate concentrations of paraoxon > 10 μM due to our interest in identifying particularly sensitive protein targets for this initial study; expanding the range of competitor in the future may help differentiate proteins that are more truly non-targets from very weak targets. Furthermore, our filtering criteria that required observations in all 3 technical replicates may have removed some proteins of interest. Future experiments including more replicates may improve target identification, particularly for lower abundance proteins.

Quantitative information about target sensitivity (e.g. IC_{50}) cannot be derived using the integral ABPP approach, but specific biochemical assays of isolated proteins are likely better suited to such detailed validation. In this study on OPs, all proteins identified through the integral

ABPP method were inhibited by the OPs over the selected concentration range, and no proteins were observed that showed increased OP-ABP labeling after OP treatment. Notably, protein targets that have opposite responses at high vs. low concentrations of competitor, such as proteins where one occupancy of an allosteric binding site influences the binding at the active site, would not be readily discernible through the integral ABPP method. In such situations, SDS-PAGE remains a low cost, rapid means to assess samples qualitatively for proteins that may display such responses, but further investigation is required to understand how those less predictable protein targets should be addressed.

In this work, we have demonstrated integral ABPP as a higher throughput chemoproteomic profiling approach that provides more information about target sensitivity than standard competitive ABPP without increasing sample numbers. The ability to profile wider concentration ranges in a higher throughput manner will advance our ability to identify potential key protein targets of diverse chemicals more rapidly and prioritize proteins of interest based on their overall sensitivity. Although not tested here, we anticipate this integral ABPP method will be applicable to other types of *in vitro* treatment samples, including live cells and fractionated samples such as microsomes or synaptosomes, which may enhance sensitivity for specific proteins that are more abundant in those subcellular fractions.

Acknowledgements

Development of the ABPP TMT workflow was supported by the Defense Threat Reduction Agency Joint Science and Technology Office for Chemical and Biological Defense under Grant Number HDTRA1-10-3-4413. Development of the integral ABPP approach was supported by a National Security Directorate Mission Seed grant under the Pacific Northwest National Laboratory (PNNL) Laboratory Directed Research and Development (LDRD) Program. We thank Ron Moore for proteomics support, and Heather Olson, Carrie Nicora, and Marina Gritsenko for proteomics sample preparation advice. We are grateful to Jordan Smith for helpful discussion. PNNL is operated by Battelle for the Department of Energy under contract DE-AC05-76RL01830.

References

1. Leung D, Hardouin C, Boger DL, Cravatt BF. Discovering potent and selective reversible inhibitors of enzymes in complex proteomes. Nat Biotechnol. 2003;21(6):687-91. Epub 20030512. doi: 10.1038/nbt826. PubMed PMID: 12740587.
2. Wang S, Tian Y, Wang M, Wang M, Sun GB, Sun XB. Advanced Activity-Based Protein Profiling Application Strategies for Drug Development. Front Pharmacol. 2018;9:353. Epub 20180409. doi: 10.3389/fphar.2018.00353. PubMed PMID: 29686618; PMCID: PMC5900428.
3. Zhu H, Sharafi M, Teh WP, Bratt AS, Buhrlage SJ, Marto JA. Strategies for Competitive Activity-Based Protein Profiling in Small Molecule Inhibitor Discovery and Characterization. Israel Journal of Chemistry. 2023;63(3-4). doi: 10.1002/ijch.202200113.
4. Casida JE, Nomura DK, Vose SC, Fujioka K. Organophosphate-sensitive lipases modulate brain lysophospholipids, ether lipids and endocannabinoids. Chem Biol Interact. 2008;175(1-3):355-64. Epub 20080520. doi: 10.1016/j.cbi.2008.04.008. PubMed PMID: 18495101; PMCID: PMC2582404.
5. Lin VS, Volk RF, DeLeon AJ, Anderson LN, Purvine SO, Shukla AK, Bernstein HC, Smith JN, Wright AT. Structure Dependent Determination of Organophosphate Targets in Mammalian Tissues Using Activity-Based Protein Profiling. Chem Res Toxicol. 2020;33(2):414-25. Epub 20200110. doi: 10.1021/acs.chemrestox.9b00344. PubMed PMID: 31872761; PMCID: PMC9014469.
6. Nomura DK, Casida JE. Activity-based protein profiling of organophosphorus and thiocarbamate pesticides reveals multiple serine hydrolase targets in mouse brain. J Agric Food Chem. 2011;59(7):2808-15. Epub 20100721. doi: 10.1021/jf101747r. PubMed PMID: 21341672; PMCID: PMC3071868.
7. Li M, Patel HV, Cognetta AB, 3rd, Smith TC, 2nd, Mallick I, Cavalier JF, Previti ML, Canaan S, Aldridge BB, Cravatt BF, Seeliger JC. Identification of cell wall synthesis inhibitors active against Mycobacterium tuberculosis by competitive activity-based protein profiling. Cell Chem Biol. 2022;29(5):883-96 e5. Epub 20211001. doi: 10.1016/j.chembiol.2021.09.002. PubMed PMID: 34599873; PMCID: PMC8964833.
8. Counihan JL, Ford B, Nomura DK. Mapping proteome-wide interactions of reactive chemicals using chemoproteomic platforms. Curr Opin Chem Biol. 2016;30:68-76. Epub 20151130. doi: 10.1016/j.cbpa.2015.11.007. PubMed PMID: 26647369; PMCID: PMC4731263.
9. Grandjean P. Paracelsus Revisited: The Dose Concept in a Complex World. Basic Clin Pharmacol Toxicol. 2016;119(2):126-32. Epub 20160624. doi: 10.1111/bcpt.12622. PubMed PMID: 27214290; PMCID: PMC4942381.
10. Desai HS, Yan T, Backus KM. SP3-FAIMS-Enabled High-Throughput Quantitative Profiling of the Cysteinome. Curr Protoc. 2022;2(7):e492. doi: 10.1002/cpz1.492. PubMed PMID: 35895291.
11. Jones HBL, Heilig R, Fischer R, Kessler BM, Pinto-Fernandez A. ABPP-HT - High-Throughput Activity-Based Profiling of Deubiquitylating Enzyme Inhibitors in a Cellular Context. Front Chem. 2021;9:640105. Epub 20210225. doi: 10.3389/fchem.2021.640105. PubMed PMID: 33718328; PMCID: PMC7947856.
12. Becker T, Wiest A, Telek A, Bejko D, Hoffmann-Roder A, Kielkowski P. Transforming Chemical Proteomics Enrichment into a High-Throughput Method Using an SP2E Workflow. JACS Au. 2022;2(7):1712-23. Epub 20220630. doi: 10.1021/jacsau.2c00284. PubMed PMID: 35911458; PMCID: PMC9326820.
13. Zecha J, Satpathy S, Kanashova T, Avanessian SC, Kane MH, Clauser KR, Mertins P, Carr SA, Kuster B. TMT Labeling for the Masses: A Robust and Cost-efficient, In-solution Labeling

Approach. Mol Cell Proteomics. 2019;18(7):1468-78. Epub 20190409. doi: 10.1074/mcp.TIR119.001385. PubMed PMID: 30967486; PMCID: PMC6601210.
14. Burton NR, Backus KM. Functionalizing tandem mass tags for streamlining click-based quantitative chemoproteomics. Commun Chem. 2024;7(1):80. Epub 20240410. doi: 10.1038/s42004-024-01162-x. PubMed PMID: 38600184; PMCID: PMC11006884.
15. Ma TP, Izrael-Tomasevic A, Mroue R, Budayeva H, Malhotra S, Raisner R, Evangelista M, Rose CM, Kirkpatrick DS, Yu K. AzidoTMT Enables Direct Enrichment and Highly Multiplexed Quantitation of Proteome-Wide Functional Residues. J Proteome Res. 2023;22(7):2218-31. Epub 20230607. doi: 10.1021/acs.jproteome.2c00703. PubMed PMID: 37285454; PMCID: PMC10337260.
16. Kalesh K, Lukauskas S, Borg AJ, Snijders AP, Ayyappan V, Leung AKL, Haskard DO, DiMaggio PA. An Integrated Chemical Proteomics Approach for Quantitative Profiling of Intracellular ADP-Ribosylation. Sci Rep. 2019;9(1):6655. Epub 20190430. doi: 10.1038/s41598-019-43154-1. PubMed PMID: 31040352; PMCID: PMC6491589.
17. Conole D, Cao F, Am Ende CW, Xue L, Kantesaria S, Kang D, Jin J, Owen D, Lohr L, Schenone M, Majmudar JD, Tate EW. Discovery of a Potent Deubiquitinase (DUB) Small-Molecule Activity-Based Probe Enables Broad Spectrum DUB Activity Profiling in Living Cells. Angew Chem Int Ed Engl. 2023;62(47):e202311190. Epub 20231017. doi: 10.1002/anie.202311190. PubMed PMID: 37779326.
18. Davison D, Howell S, Snijders AP, Deu E. Activity-based protein profiling of human and plasmodium serine hydrolases and interrogation of potential antimalarial targets. iScience. 2022;25(9):104996. Epub 20220824. doi: 10.1016/j.isci.2022.104996. PubMed PMID: 36105595; PMCID: PMC9464883.
19. Gaetani M, Sabatier P, Saei AA, Beusch CM, Yang Z, Lundstrom SL, Zubarev RA. Proteome Integral Solubility Alteration: A High-Throughput Proteomics Assay for Target Deconvolution. J Proteome Res. 2019;18(11):4027-37. Epub 20191014. doi: 10.1021/acs.jproteome.9b00500. PubMed PMID: 31545609.
20. Wiedner SD, Burnum KE, Pederson LM, Anderson LN, Fortuin S, Chauvigne-Hines LM, Shukla AK, Ansong C, Panisko EA, Smith RD, Wright AT. Multiplexed activity-based protein profiling of the human pathogen Aspergillus fumigatus reveals large functional changes upon exposure to human serum. J Biol Chem. 2012;287(40):33447-59. Epub 20120803. doi: 10.1074/jbc.M112.394106. PubMed PMID: 22865858; PMCID: PMC3460446.
21. Keith S, Williams M, Fay M, Wilson JD, Llados F, Carlson-Lynch H, Wohlers D, Hard C, Citra M. Toxicological profile for parathion. 2017.
22. Wolejko E, Lozowicka B, Jablonska-Trypuc A, Pietruszynska M, Wydro U. Chlorpyrifos Occurrence and Toxicological Risk Assessment: A Review. Int J Environ Res Public Health. 2022;19(19). Epub 20220926. doi: 10.3390/ijerph191912209. PubMed PMID: 36231509; PMCID: PMC9566616.
23. Silberman J, Taylor A. Carbamate Toxicity. StatPearls. Treasure Island (FL): StatPearls Publishing

24. Kim S, Pevzner PA. MS-GF+ makes progress towards a universal database search tool for proteomics. Nat Commun. 2014;5:5277. Epub 20141031. doi: 10.1038/ncomms6277. PubMed PMID: 25358478; PMCID: PMC5036525.
25. Monroe ME, Shaw JL, Daly DS, Adkins JN, Smith RD. MASIC: a software program for fast quantitation and flexible visualization of chromatographic profiles from detected LC-

MS(/MS) features. Comput Biol Chem. 2008;32(3):215-7. Epub 20080226. doi: 10.1016/j.compbiolchem.2008.02.006. PubMed PMID: 18440872; PMCID: PMC2487672.
26. Long JZ, Cravatt BF. The metabolic serine hydrolases and their functions in mammalian physiology and disease. Chem Rev. 2011;111(10):6022-63. Epub 20110623. doi: 10.1021/cr200075y. PubMed PMID: 21696217; PMCID: PMC3192302.
27. Lenfant N, Bourne Y, Marchot P, Chatonnet A. Relationships of human alpha/beta hydrolase fold proteins and other organophosphate-interacting proteins. Chem Biol Interact. 2016;259(Pt B):343-51. Epub 20160421. doi: 10.1016/j.cbi.2016.04.027. PubMed PMID: 27109753.
28. Fujioka K, Casida JE. Glutathione S-transferase conjugation of organophosphorus pesticides yields S-phospho-, S-aryl-, and S-alkylglutathione derivatives. Chem Res Toxicol. 2007;20(8):1211-7. Epub 20070721. doi: 10.1021/tx700133c. PubMed PMID: 17645302.
29. de Graaf EL, Pellegrini D, McDonnell LA. Set of Novel Automated Quantitative Microproteomics Protocols for Small Sample Amounts and Its Application to Kidney Tissue Substructures. J Proteome Res. 2016;15(12):4722-30. Epub 20161110. doi: 10.1021/acs.jproteome.6b00889. PubMed PMID: 27809536.
30. Guo Y, Yu D, Cupp-Sutton KA, Liu X, Wu S. Optimization of protein-level tandem mass tag (TMT) labeling conditions in complex samples with top-down proteomics. Anal Chim Acta. 2022;1221:340037. Epub 20220607. doi: 10.1016/j.aca.2022.340037. PubMed PMID: 35934336; PMCID: PMC9371347.
31. Stepath M, Zulch B, Maghnouj A, Schork K, Turewicz M, Eisenacher M, Hahn S, Sitek B, Bracht T. Systematic Comparison of Label-Free, SILAC, and TMT Techniques to Study Early Adaption toward Inhibition of EGFR Signaling in the Colorectal Cancer Cell Line DiFi. J Proteome Res. 2020;19(2):926-37. Epub 20200114. doi: 10.1021/acs.jproteome.9b00701. PubMed PMID: 31814417.
32. Harris L, Fondrie WE, Oh S, Noble WS. Evaluating Proteomics Imputation Methods with Improved Criteria. J Proteome Res. 2023;22(11):3427-38. Epub 20231020. doi: 10.1021/acs.jproteome.3c00205. PubMed PMID: 37861703; PMCID: PMC10949645.
33. O'Connell JD, Paulo JA, O'Brien JJ, Gygi SP. Proteome-Wide Evaluation of Two Common Protein Quantification Methods. J Proteome Res. 2018;17(5):1934-42. Epub 20180419. doi: 10.1021/acs.jproteome.8b00016. PubMed PMID: 29635916; PMCID: PMC5984592.
34. Strickland KE. Interspecies Differences in Organophosphate Anticholinesterase Inhibition Potency and Reactivation Using Novel Oximes: Mississippi State University; 2023.
35. Nomura DK, Hudak CS, Ward AM, Burston JJ, Issa RS, Fisher KJ, Abood ME, Wiley JL, Lichtman AH, Casida JE. Monoacylglycerol lipase regulates 2-arachidonoylglycerol action and arachidonic acid levels. Bioorg Med Chem Lett. 2008;18(22):5875-8. Epub 20080806. doi: 10.1016/j.bmcl.2008.08.007. PubMed PMID: 18752948; PMCID: PMC2593629.
36. Jokanovic M, Kosanovic M, Maksimovic M. Interaction of organophosphorus compounds with carboxylesterases in the rat. Arch Toxicol. 1996;70(7):444-50. doi: 10.1007/s002040050297. PubMed PMID: 8740539.
37. Maxwell DM. The specificity of carboxylesterase protection against the toxicity of organophosphorus compounds. Toxicol Appl Pharmacol. 1992;114(2):306-12. doi: 10.1016/0041-008x(92)90082-4. PubMed PMID: 1609424.
38. Lian J, Nelson R, Lehner R. Carboxylesterases in lipid metabolism: from mouse to human. Protein Cell. 2018;9(2):178-95. Epub 20170704. doi: 10.1007/s13238-017-0437-z. PubMed PMID: 28677105; PMCID: PMC5818367.

536